A Single Finger Geometry Recognition Based On Widths And Fingertip Angles (WFTA)

Mohd Shahrimie Mohd Asaari
Intelligent Biometric Group,
School of Electrical & Electronic Eng.,
Universiti Sains Malaysia, 14300,
Nibong Tebal, Penang, Malaysia.
mohdshahrimie@yahoo.com

Bakhtiar Affendi Rosdi
Intelligent Biometric Group,
School of Electrical & Electronic Eng.,
Universiti Sains Malaysia, 14300,
Nibong Tebal, Penang, Malaysia.
eebakhtiar@eng.usm.my

Abstract

We proposed a new geometric feature representation for the infrared finger image recognition system. The geometric representation is based on the fusion of two types of features, which are the finger widths and the fingertip angles. The extracted finger widths and fingertip angels are transformed into frequency domain using Discrete Fourier Transform (DFT) to make them robust to the shifting and rotation variations. The feature sets obtained from the DFT process are fused by concatenating them into a single row vector called width and fingertip angle (WFTA) feature. To ensure the orthogonal relationship between the WFTA components, the Principle Component Analysis is adopted at the matching stage. Experimental results show that recognition accuracy is significantly enhanced using the proposed method.

1 Introduction

In the past two decades, researchers invested a lot of efforts to develop different techniques to recognize human identity based on hand geometry features. Typical examples of these features include finger lengths, finger widths, finger heights at the knuckle positions, palm width, finger perimeters, finger areas and aspect ratio of the palm to fingers. For example, Kumar et al. [1] present a hand recognition system based on four finger lengths, eight finger widths (two widths per finger), palm width, palm length, hand area, and hand length. Boreki et al. [2] extract the angle between the differences of slopes on all the contour of the segmented hand image. Veldhuis et al. [3] develop a hand geometry recognition based on the contour-based features. They extract the spatial coordinates of certain landmarks on the contour and measurement of the lengths and angels of the line segments are used as the geometric features. The work described in [4] uses the distances from wrist reference to the fingertips and finger valleys as the geometric features. The previous hand geometry recognition methods extracted the geometric features of the overall hand shape using landmarks such as fingertip points and the valley points between adjacent fingers. Thus, the size of the capturing device is big.

In recent years, several researchers have put their efforts to develop finger geometry recognition on infrared finger image based on a single finger [5, 6, 7, 8]. These efforts are made for developing multimodal finger based biometrics that combined the finger geometry with other biometrics information such as the vein patterns and the finger prints. They use the input image from a single finger and the capturing device is constructed as a tiny device which can acquire all the biometrics information at the same time. However, for the finger geometry recognition, they use only the finger widths as the geometric features. Therefore, their recognition accuracy does not guarantee a promising result because the single-feature type usually lack of distinctiveness of the biometric trait [9].

To address the above-mentioned problems, we propose to integrate two types of geometry features at the feature level fusion. Compared to the single geometry feature, multi-features contain richer information about the finger geometry. Therefore, integrating multiple features will improve the matching accuracy. In this study, we extract two types of geometric features, which are the finger width [5, 6, 7] and our newly proposed feature, the so-called fingertip angle. To make the extracted features robust to the shifting and rotation error, the features are transformed into Fourier descriptors (FDs) and normalized to their respective DC component [6]. Then, the widths and fingertip angles are fused by a simple concatenation of the features sets obtained from the FD transformation thus producing a new feature vector called width and fingertip angle (WFTA). Finally, the PCA is used to enhance the orthoganality between the WFTA components.

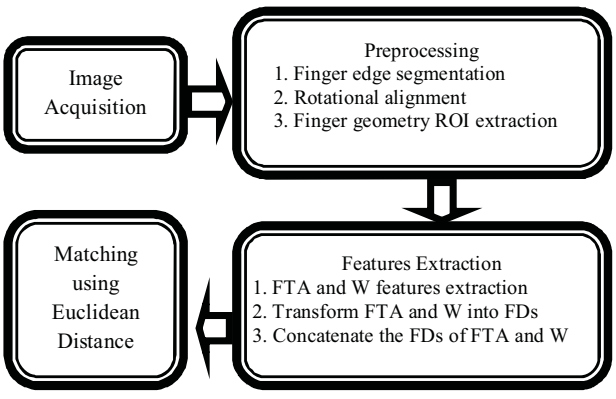

Figure 1. Block diagram of the proposed finger geometry recognition system.

2 Proposed Method

Figure 1 shows the diagram of the proposed system that consists of four main processes which are the image acquisition, preprocessing, features extraction and finger matching.

2.1 Image acquisition

Figure 2 shows the image of the capturing device of our proposed system. This device consists of three units of Near-Infrared Light Emitting Diode (NIR-LED) with 850 nm wavelength and a Sony PSEye camera with an IR passing filter. The NIR-LEDs are placed in a row on top section while the camera is attached at the bottom side of the capturing device. This device can acquire the finger vein patterns and the finger geometry information at the same time. However, in this paper we only focus on the geometry information that is used to develop finger geometry recognition as this is our initial study towards a finger based multi-modal biometric system.

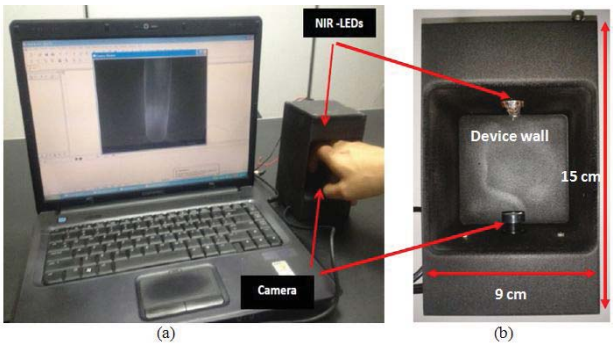

Figure 2. The proposed infrared finger image capturing device:(a) image acquisition procedure and (b) image capturing device.

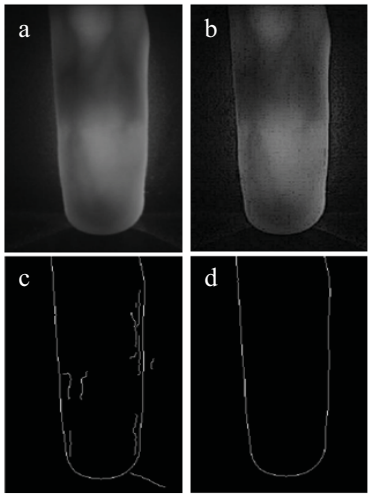

Figure 3. (a) is the original image,(b) is the enhanced image using Laplacian filter, (c) is the extracted lines by the Canny edge's operator, and (d) is the final image after applying the connected-component labeling.

2.2 Preprocessing

There are three major steps in the preprocessing stage, which are finger edge segmentation, rotational alignment and region of interest (ROI) extraction. In finger edge segmentation procedure, a 3×3 Laplacian mask filter [10] is applied to enhance the edge of the finger image. Then, the finger edge line is extracted using the Canny edge detector technique [11]. However, we found that the result of the Canny edge's operator still producing a number of undesirable edge lines. Therefore, a proper connected-component labeling [12] is applied to discard the unwanted edge lines. Figure 3 shows the result of finger edge segmentation after applying the Canny edge operator and connected-component labeling technique.

In order to reduce the recognition errors caused by rotation of the finger, a rotation alignment is carried out. In this procedure, the fingertip is first detected by locating the horizontal fingertip point y_{ft} based on the estimated point from the end point of the bottom side of the finger edge image. Then, the vertical fingertip point x_{ft} is estimated by measuring the center position of two end points (x_l and x_r) which located d distance (40 pixels) from the horizontal line of fingertip as shown in Figure 4. The center line of the finger region is drawn by calculating the mean values of the x positions of the right and left finger boundaries at each y position along Δy from the horizontal line of fingertip [7]. In our system, Δy is set to 380 pixels and the rotation angle θ is calculated as

$$\tan\theta = \frac{\Delta x}{\Delta y} = \frac{x_{ft} - x}{y_{ft} - y} \tag{1}$$

where (x, y) and (x_{ft}, y_{ft}) denote the points on the center line and the fingertip points, respectively and Δx is the different between x_{ft} and x.

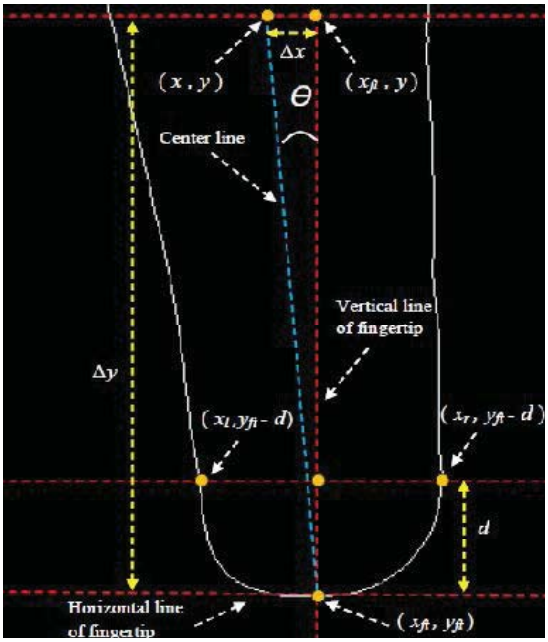

Figure 4. Measuring the fingertip center line and rotation angle.

The captured infrared finger images are sometimes hampered by shaded regions at both top and bottom areas due to improper finger placement during the enrolment process. To exclude the inaccurate geometry information, we define the final geometry ROI where the edge lines at top and bottom ends are discarded leaving the right and left edges along the area of M pixels length as shown in Figure 5. In this procedure, the discarded parts at the top and bottom regions are set

empirically, where they start at a distance of 320 and 40 pixels from the fingertip point, respectively. Hence, in our work, M is equal to 280 pixels.

2.3 Features Extraction

In this procedure, two types of geometry features are extracted, which are the finger width (W) and our newly proposed geometry feature called fingertip angle (FTA). The finger width vectors, i.e., $w = [w_0, w_1, w_2, w_3, ..., w_j]$ are measured to represent the finger shape, and they are extracted at the equal step intervals along the finger length of M pixels. On the other hand, the FTA features present the angles between the center line and the line segments that connecting the fingertip and the boundary points. Since the finger geometry consists of two edge lines, i.e., the right contour and the left contour, the FTA features are calculated at both sides. Following the same step interval for the finger widths calculation, which is set to one pixel, the FTA for the right side, i.e., $ftar = [\theta r_0, \theta r_1, \theta r_2, \theta r_3, ..., \theta r_j]$ and the left side, i.e., $ftal = [\theta l_0, \theta l_1, \theta l_2, \theta l_3, ..., \theta l_j]$ provide the same number of feature vectors as shown in Figure 5. Prior combining both W and FTA features, their feature vectors are transformed into Fourier descriptors (FDs) [6] using Discrete Fourier Transform (DFT). The FDs represent the geometry information of a single finger in the frequency domain. In all, we have three FD vectors, which are given by

$$G_W = [\frac{W_1}{W_0}, \frac{W_2}{W_0}, \frac{W_3}{W_0}, ... \frac{W_j}{W_0}]^T \quad (2)$$

$$G_{\theta R} = [\frac{\theta R_1}{\theta R_0}, \frac{\theta R_2}{\theta R_0}, \frac{\theta R_3}{\theta R_0}, ... \frac{\theta R_j}{\theta R_0}]^T \quad (3)$$

$$G_{\theta L} = [\frac{\theta L_1}{\theta L_0}, \frac{\theta L_2}{\theta L_0}, \frac{\theta L_3}{\theta L_0}, ... \frac{\theta L_j}{\theta L_0}]^T \quad (4)$$

where, G_W is the FD vector of finger widths, $G_{\theta R}$ and $G_{\theta L}$ are the FD vectors of fingertip angles for right and left side, respectively. In addition, $W_i, \theta R_i, \theta L_i$ denote the ith component and $W_0, \theta R_0, \theta L_0$ denote the DC component of each FD vector in the frequency domain, respectively. Finally, all the three FD vectors are fused together by concatenating them into a single row vector as

$$G = [G_{\theta R}, G_{\theta L}, G_W]^T \quad (5)$$

where, G is the final FD vector representing the WFTA features in the frequency domain.

2.4 Finger Matching

As suggested in [7], the orthogonality between the FDs component can be enhanced by adopting a linear transformation method based on PCA technique. In this procedure, the so-called scatter matrix S is calculated as

$$S = \sum_{i=1}^{N} [G_i - \bar{G}] - [G - \bar{G}]^T \quad (6)$$

where, $\bar{G}$ denotes the mean vector of the FDs on the training dataset. The eigenvector e_i and eigenvalue λ_i are obtained by

$$Se_i = \lambda_i e_i, \quad i = 1, 2, 3, ...N \quad (7)$$

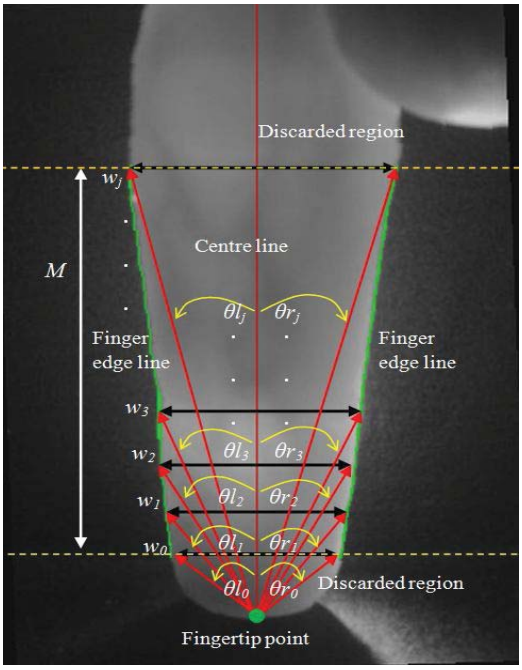

Figure 5. Measuring the finger widths and fingertip angles.

where, N is the total number of finger images in the training set. The score of the finger geometry recognition is finally measured by calculating the Euclidean distance, ED between the eigenvalues of the enrolled and input FDs as

$$ED = \frac{1}{m-1} \sqrt{\|\lambda_A - \lambda_B\|}^2 \quad (8)$$

where, λ_A and λ_B denote the vectors of eigenvalues of the enrolled and input FDs, respectively. m denotes the number of eigenvalues. In this procedure, the m value is obtained empirically, where based on the first 75% of the total eigenvalues, the lowest EER is achieved.

3 Experimental Results

To evaluate the performance of proposed algorithm, we developed an infrared finger image database from 123 volunteers ranged from 20 to 52 years old. Every volunteer provides four fingers, which are the index and middle fingers from both left and right sides resulting a total of 492 finger classes are collected. The finger images are captured using the capturing device as shown in Figure 2. The images are collected in two sessions separated more than two weeks time. In each session, the same finger is captured 6 times. Therefore, there is a total of 2952 (492×6) images in the database. The images in the first session are defined to be the registered set, while the images in the second session are used as the testing set. Therefore, we have a total of 17,712 ($492 \times 6 \times 6$) genuine matches and 8,696,592 ($(492 \times 492 \times 6) - 17712$) impostor matches. The recognition performance is evaluated based on Equal Error Rate (EER), which is defined as the error rate when the False Acceptance Rate (FAR) and the False Rejection Rate (FRR) are equal. FRR is the error rate

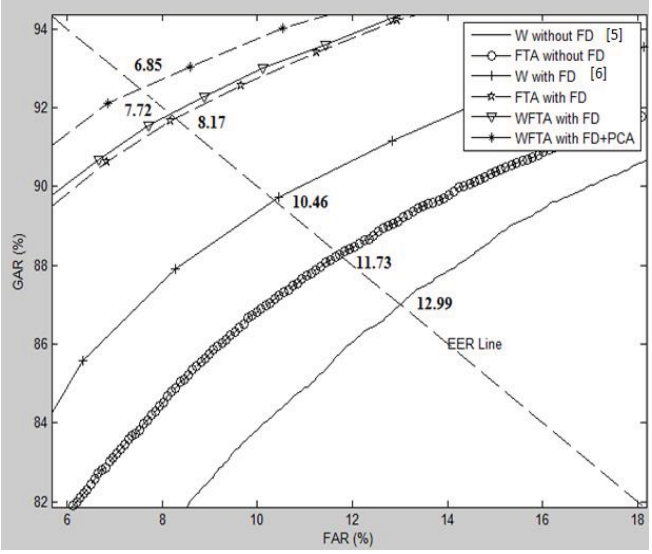

Figure 6. Experimental results described in terms of ROC curves and EER plot.

when the enrolled finger vein images are rejected as un-enrolled images and FAR is the error rate when the un-enrolled finger vein images are accepted as enrolled images.

Figure 6 shows the receiver operating characteristic (ROC) curves of our experimental results, where Genuine Acceptance Rate (GAR) is defined as GAR = 100% - FRR. Without applying the FD transformation, it is observed that the recognition results for W and FTA features produced lower accuracy with EER of 12.99% and 11.73%, respectively. These unconvincing results are due to the both features are very sensitive to small segmentation errors caused by the shifting and rotation of the finger. The aforementioned problem is solved by transformed the geometry features into frequency domain using DFT where the EER for W and FTA are decreased to 10.46% and 8.17% respectively. We also observe that in both conditions (i.e., with or without FD transformation) the recognition result for FTA is better than the W feature. But, relaying on the single feature type is still insufficient to discriminate all finger classes. Therefore, applying the information fusion is considered an acceptable strategy in order to complement each W and FTA features. In the proposed method, the FDs of W and FTA vectors have been normalized to their DC component. Hence, their feature set are located into a common range. Therefore, consolidating them in the feature level is possible. The ROC curve (WFTA with FD) shows that the fusion of both geometry features has improved the recognition accuracy where the EER is reduced by as much as 2.74% and 0.45% compared with single W and FTA features, respectively. The improvement is believed due to the fact that multi-features contain richer description of the finger geometry information, therefore, it can provide better recognition results. However, the accuracy of WFTA fusion still can be further enhanced because orthogonality between the FDs is not guaranteed. Therefore, in our final solution, the PCA is used. As shown by the ROC curve (WFTA with FD+PCA), our final proposed method produces the best recognition accuracy with the EER of 6.85%.

4 Conclusion

In this work, we developed a new approach of finger geometry recognition using the combination of finger width and fingertip angle features. The finger widths and the fingertip angles are transformed into FDs to make them robust to the translation and rotation of the finger. The fusion of finger widths and fingertip angles based on FDs achieved better recognition accuracy than single-feature techniques. The finger geometry recognition was greatly improved by combining the FDs of WFTA features with the PCA method. In the future, we plan to combine the proposed finger geometry features with finger vein to produce a robust multi-modal finger based biometrics system.

Acknowledgements

This work is supported by Universiti Sains Malaysia Research University Grant No. 1001/PELECT/814116 and Post Graduate Incentive Grant No. 1001/PELECT/8023013.

References

[1] A. Kumar, D. Wong, H. Shen, A. Jain, Personal verification using palmprint and hand geometry biometric, Proceeding of the Audio-and Video-Based Biometric Person Authentication, pp.1060–1060, 2003.

[2] G. Boreki, A. Zimmer, Hand geometry: a new approach for feature extraction, Proceeding of the Fourth IEEE Workshop on Automatic Identification Advanced Technologies, pp.149–154, 2005.

[3] R. Veldhuis, A. Bazen, W. Booij, A. Hendrikse, Hand-geometry recognition based on contour landmarks, From Data and Information Analysis to Knowledge Engineering, pp.646–653, 2006.

[4] E. Yoruk, E. Konukoglu, B. Sankur, J. Darbon, Shape-based hand recognition, IEEE Transactions on Image Processing, vol.15, no.7, pp.1803–1815, 2006.

[5] B. Kang, K. Park, Multimodal biometric authentication based on the fusion of finger vein and finger geometry, Optical Engineering, vol.(48), pp.090501, 2009.

[6] B. Kang, K. Park, Multimodal biometric method based on vein and geometry of a single finger, IET Computer Vision, vol.4, no.3, pp.209–217, 2010.

[7] B. Kang, K. Park, J. Yoo, J. Kim, Multimodal biometric method that combines veins, prints, and shape of a finger, Optical Engineering, vol.50, pp.017201, 2011.

[8] E. Lee, H. Jung, D. Kim, New finger biometric method using near infrared imaging, Sensors, vol.11, no.3, pp. 2319–2333, 2011.

[9] A. Ross, R. Govindarajan, Feature level fusion of hand and face biometrics, Proceeding of the Defense and Security, pp.196–204, 2005.

[10] R. Gonzales, R. Woods, S. Eddins, Digital Image Processing Using Matlab, Prentice Hall, Upper Saddle River, New Jersey, 2004.

[11] J. Canny, A computational approach to edge detection, IEEE Transactions on Pattern Analysis and Machine Intelligence, vol.6, pp.679–698, 1986.

[12] M. Dillencourt, H. Samet, M. Tamminen, A general approach to connected-component labeling for arbitrary image representations, Journal of the ACM, vol. 39, no.2, pp.253–280, 1992.